# 連続フレーム画像を用いた反射パラメータの推定法

張　暁華*　中西　良成*　小林　希一*　三ッ峰　秀樹**　齋藤　豪***
*NHK　エンジニアリングサービス
**NHK 放送技術研究所
***東京工業大学精密工学研究所

# Estimation of Surface Reflectance Parameters from Image Sequence

Xiaohua Zhang*　Yoshinari Nakanishi*　Kiichi Kobayashi*
Hideki Mitsumine**　Suguru Saito***
*NHK Engineering Services Inc.
**NHK Science and Technical Research Laboratories
**Tokyo Institute of Technology

## Abstract

We had developed an approach for estimating diffuse and specular reflectance parameters of 3D object from image sequence taken by a high definition TV camera with fixed position and direction, and the light source direction is also fixed while the object is rotating on a rotary table. There are many researchers had done this kind of research work for computing reflectance parameters from the separated diffuse component and specular component. However, in the case of complicated texture, the separation is very difficult or incomplete. Unlike the other methods, our approach estimates diffuse and specular parameters directly from the raw RGB data by iteratively minimizing fitting errors without knowing light source color and object color signal. The diffuse component and specular component can be separated using the estimated diffuse and specular reflectance parameters. The experimental results for both synthesized and real data demonstrate that the proposed approach recovers the reflectance parameters effectively and stably.

## 1. Introduction

Object reflectance properties had become more important in order to acquire object model and object texture for generating highly realistic synthesized images in computer graphics applications such as virtual reality, virtual museums and virtual studio. The research on object reflectance properties has attracted many researchers in computer vision community to devote their forces on it. At the early time, the research was emphasized on the color space analysis for image segmentation by partitioning a color histogram into clusters. There are several papers handling reflectance using dichromatic reflectance model to describe the illumination of a uniformly colored object in color space [1,2] for separating diffuse reflection component and specular reflection component. The separated components are used for segmentation of color image without suffering from the disturbances of highlight in the images [3]. However, since this method is based on the assumption that the object is uniformly colored, it cannot handle the reflectance from object with complex texture.

The technique of separation of diffuse and specular components by applying a polarization filter has also been researched. The reference [4] introduced a technique to separate diffuse and specular components of a reflectance object with complex texture by using polarization and produced very impressive experimental results under assumption that the diffuse reflection component is un-polarized, the algorithm needs some priori knowledge in choosing thresholds for parameter estimation.

There are also other techniques such as shape from shading [5, 6] and photometric stereo [7,8] for analyzing images to recover the surface reflectance properties along with the surface shape under the assumption that the real object is Lambertian.

Recovering reflectance properties of object from color image sequence has been proposed by using the concept of temporal color space [9] and applied successfully for object shape and reflectance modeling [10]. This method first separates the diffuse and specular components and then computes the reflectance from the separated components with known calibrated specular color vector and measured diffuse reflection color.

Unlike the methods mentioned above, we estimate reflectance properties directly from the image sequence to alleviate the errors during separation. The computed diffuse and specular reflectance properties are then used for separating the two components. The estimation of reflectance properties is done, by applying an iterative algorithm to fit the color values from different views to a nonlinear reflection model for each 3D point on the surface. This is more effective and stable since the fitting is based on the raw RGB data for computing all parameters in the model.

This report is organized as follows: Section 2 explains the experimental setup for obtaining color image sequence. Section 3 describes the reflection model and the iterative nonlinear fitting algorithm for estimating reflectance properties and separating the two reflection components. Section 4 shows our impressive experimental results of diffuse component and specular component using the computed reflectance properties and section 5 gives the conclusion and the future work.

## 2. The experimental setup

The experimental setup of image acquisition system is illustrated in Figure 1. The object whose reflectance properties are to be estimated is mounted on a rotary table. The rotation is controlled with a PC. The rotating direction is shown in the figure. The position and orientation of a HDTV camera relative to the rotary table are fixed. The point light source direction is also fixed, which can be measured under the assumption that the light is far enough to the object. It means that the distance between light source and object is larger enough than the size of object.

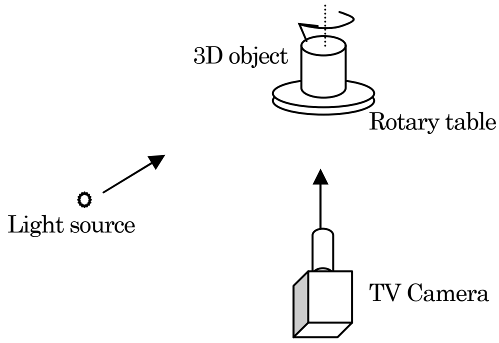


Figure 1. The experimental setup

A color image sequence is taken using this setup, by rotating the 3D object around the rotation axis at a fixed angle step such as 2 degree, then the sequence contains 180 images. We simply use a single incandescent lamp as the light source. Only the light source direction needs to be measured. We do not need the light source color be calibrated, which is different with the approach introduced in [9, 10]. For each point on the 3D object, the corresponding RGB values on each image can be taken by modeling approaches, using the calibrated camera intrinsic and extrinsic parameters [11].

## 3. Reflectance properties estimation

The reflection from a 3D point is related to the normal of this point, light direction and view direction. The variation of reflection from all angles provides us to compute the reflectance properties. When the RGB data of each point on the 3D object are prepared, the reflectance properties can be analyzed. The estimation is performed basically for each pixel independently from neighboring pixels. In our implementation, we use a small window to alleviate the random noise under the assumption that the variation of intensities is continuous.

### 3.1. Reflectance modeling

Figure 2 shows the geometry configuration of our experimental setup. The optical axis of the camera is collinear with $z$ axis and the rotation axis of rotary table is collinear with $y$ axis. The vector $n$ is the normal of a 3D point on the object surface and $L$ is the direction of point light source. Vector $L'$ and $n'$ are the projection of $L$ and $n$ on to $XOZ$ plane. $\varphi_L$ is the angle between the light source and $y$ axis; $\theta_L$ is the angle between the projection $L'$ of $L$ and $z$ axis. The light source direction $\varphi_L$ and $\theta_L$ can be measured in advance. $\varphi_n$ is the angle between normal and $y$ axis; $\theta_n$ is the angle between the projection of normal vector and $z$ axis.

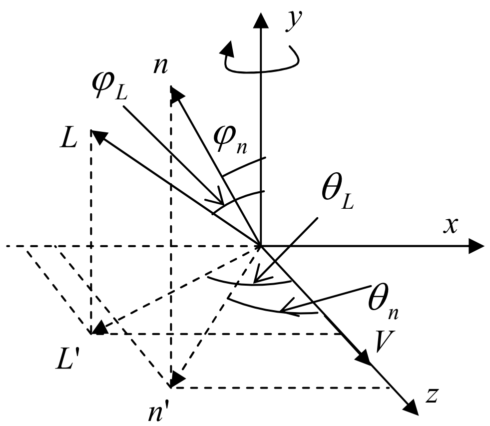


Figure 2. Geometry configuration

Since the object surface reflectance can be modeled as the linear combination of diffuse component and specular component for each channel, we use the simplified Torrance -Sparrow model [12] to describe this combination in following equation:

$$\begin{aligned} I &= I_d + I_s \\ &= K_d(L \cdot n) + K_s e^{-\alpha^2/2\sigma^2} \end{aligned} \quad (1)$$

Here $L \cdot n$ is the inner product of two vectors. $K_d$ is the diffuse reflection parameter and $K_s$ is the specular reflection parameter. Parameter $\alpha$ is the angle between surface normal and the bisector of the light source direction and view direction. $\sigma$ is the standard deviation of a facet slope of the Torrance-Sparrow model. Let the surface normal be $n = (p, q, r)$. Since the light source direction is fixed and the object is rotating, it also can be considered as that the object is fixed and the light source is rotating around the same rotation axis. Therefore, parameter $\theta$ and $\alpha$ are regarded as variable and other parameters are fixed. We rewrite $\theta_L$ as $\theta$ and equation (1) is reformed as following function for each 3D point:

$$\begin{aligned} I = {} & A \sin\varphi_L \sin\theta + \\ & B\cos\varphi_L + C\sin\varphi_L\cos\theta + De^{-\left(\frac{E-\theta}{F}\right)^2} \end{aligned} \quad (2)$$

What we need to estimate is the parameters in the above equation: $A = K_d p$, $B = K_d q$, $C = K_d r$, $D = K_s$, $E$ and $F = \sqrt{2}\sigma$. After the parameters in equation (2) are computed, the reflection parameter $K_d$ and surface normal are calculated using following equations. Note that the surface normal is normalized.

$$\begin{aligned} K_d &= \sqrt{A^2 + B^2 + C^2} \\ p &= A / K_d \\ q &= B / K_d \\ r &= C / K_d \end{aligned} \quad (3)$$

Moreover the two angles of surface normal as shown in figure 2 can also be computed:

$$\begin{aligned} \theta_n &= \cos^{-1}\left(\frac{r}{\sqrt{p^2 + r^2}}\right) \\ \varphi_n &= \cos^{-1}\left(\frac{q}{\sqrt{p^2 + q^2 + r^2}}\right) \end{aligned} \quad (4)$$

The specular reflection parameter $K_s$ is the same as the parameter $D$ and the standard deviation $\sigma = F / \sqrt{2}$. Since 6 parameters are unknown in the equation (2), mathematically we need at least 6 samples from 6 frames to fit the intensity variation.

### 3.2. Parameter fitting

In order to estimate each parameter in equation (2) on each channel, our technique minimize the sum of the squared intensity errors over all corresponding pixels on each view as shown the following equation:

$$Err = \sum_k (I(\theta_k; A, B, C, D, E, F) - I_k)^2 = \sum_k e_k \quad (5)$$

This nonlinear minimization problem is solved in our implementation by applying Levenberg Marquardt iterative method [13]. This method needs taking the first derivatives of error respect to each unknown parameter. For example, the first derivative of error with respect to $F$ is as (6).

$$\frac{\partial e_k}{\partial F} = -2De^{-\left(\frac{E-\theta}{F}\right)^2} \cdot \left(\frac{E-\theta}{F}\right)^2 \cdot \frac{1}{F} \qquad (6)$$

From these first derivatives, the approximate symmetrical Hessian matrix $P = \lfloor p_{ij} \rfloor$ and the weighted gradient vector $Q = \{q_i\}$ is computed with components as in the following equations:

$$p_{ij} = \sum_k \frac{\partial e_k}{\partial m_i} \frac{\partial e_k}{\partial m_j} \quad q_i = -2\sum_k e_k \frac{\partial e_k}{\partial m_i} \qquad (7)$$

Where $m_i$ and $m_j$ represent the parameters *A, B, C, D, E* and *F* in function (2). The nonlinear problem now becomes a linear algebra problem to compute the increment of parameters:

$$(P + \lambda I)\Delta m = Q \qquad (8)$$

Here $\lambda$ is a time varying stabilization parameter which is set to be 0.0001 as recommended in [13]. Solving the system (8) and updating the parameters $m_i$ iteratively until either the error is below a threshold or a fixed number of steps have been completed will give us the final value of parameters as

$$m^{t+1} \leftarrow m^t + \Delta m \qquad (9)$$

Unfortunately, this nonlinear iterative method only finds the locally optimal solution. This means that the minimization needs a good initial guess for each parameter. With bad initial guess, the algorithm may not converge to the expected solution. In our implementation, we determine the initial guess for parameters using following method. The initial *D* value is the peak value in the measured data for each 3D point. The initial *E* value is the position of the peak. The initial F value is empirically given between 0.01 and 1.0. We use 0.08 as initial parameter *F* value in the implementation. The initial values of *A, B,* and *C* are treated as the same: the value whose position is far away from the peak in the measured data. This method is something similar to the method in [9] for computing body color vector, since the peak is considered to be approximate to the light source color vector. However, the difference is that we do not fix the body color vector and light source color vector. These vectors will be refined in the algorithm, because that the initial guess is not accurate enough for some reasons such as noise, measurement error and environment light etc.

### 3.3. Separating the two components

When the parameters in function (2) are estimated, the reflectance properties and surface normal can be computed as equation (3) and (4). We have three solutions for the surface normal from three channels. Since the surface normal is invariant with each channel, these solutions are averaged as the final normal. The mean of Gaussian distribution and the standard deviation of the facet slope of a 3D point are intrinsic. Therefore we also compute their average value from the solution of three channels. Using the parameter values estimated, the diffuse reflection and specular reflection components of reflection in equation (2) is computed:

$$I'_d = K_d(p\sin\varphi_L \sin\theta + q\cos\varphi_L + r\sin\varphi_L \cos\theta)$$
$$I'_s = K_s e^{-(\frac{E-\theta}{F})^2} \qquad (10)$$

Then the separated diffuse component and specular component of original reflectance are:

$$I_d = I * \frac{I'_d}{I'_d + I'_s} \quad I_s = I * \frac{I'_s}{I'_d + I'_s} \qquad (11)$$

Since the two components of equation (10) are computed from the model that has error with the original data, we use the results of equation (11) as the separated diffuse and specular reflection components, in which some failure points are interpolated from neighbor pixels.

### 3.4. Summary of algorithm

The following is the summary of the proposed algorithm for estimating the reflectance properties and the object shape, separating the diffuse reflection and specular reflection components from the original reflection data. The inputs are the color data taken for a surface point with the corresponding pixel on the image sequence and the light direction. The outputs are reflectance properties, object shape and the separated diffuse and specular reflection components.

The algorithm loops on the following steps over each surface point:

① Compute the initial guess for each fitting parameter in equation (2);

② Estimate the optimal parameters for minimizing the fitting error (5);

③ Compute the reflectance properties and surface normal;

④ Calculate the reflection components from the original data using the computed reflectance properties and surface normal.

The advantage of using Levenberg Marquardt over straightforward gradient descent is that it converges in less iteration.

## 4. Experimental Results

The experimental system arrangement is illustrated in figure 1 as described in section 2.

Table 1. Simulation result

| | Parameter values used for synthesis | Estimated parameter values |
|---|---|---|
| $K_{dr}$ | 0.777543 | 0.7775430 |
| $K_{dg}$ | 0.392522 | 0.3925219 |
| $K_{db}$ | 0.491277 | 0.4912774 |
| $K_{sr}$ | 0.498124 | 0.4981243 |
| $K_{sg}$ | 0.586319 | 0.5863187 |
| $K_{sb}$ | 0.638829 | 0.6388292 |
| $\theta_L$ | 35.0° | |
| $\phi_L$ | 85.0° | |
| $\theta_n$ | 10.0° | 10.034438° |
| $\phi_n$ | 90.0° | 90.000583° |
| $\sigma$ | 0.05 | 0.0500175 |

Our experiments are performed on synthesized data and the real data obtained from the image sequence. In order to verify the proposed algorithm for estimating reflectance properties, we synthesized a group of data using the mechanism similar to the experimental setup. The simulation results are shown in table 1. Here, $K_{dr}$, $K_{dg}$, $K_{db}$ and $K_{sr}$, $K_{sg}$, $K_{sb}$ are diffuse and specular reflection parameters in RGB channels respectively. The other parameters are as illustrated as in figure 2 or as explained as in section 3. We know that, from the table 1, the estimated values are very close to the synthesis values. The curves of synthesized data in each channel are shown in figure 3 (a). The curves of separated two components using the proposed algorithm are shown in figure 3 (b).

In the experiment with real data, we have taken a sequence of images of a vase with complicated texture on it. The camera and light source are fixed while the 3D object mounted on a rotary table and rotated around the rotation axis. The RGB intensities of all surface points are obtained using modeling method. Currently, in this experiment, although we had taken 180 image frames around the object, for each 3D point on the object, we took the sampled RGB data from 31 frames with 4° interval.

Figure 4 (a) shows one of image from the image sequence. We first estimate the reflectance parameters and then separate the two components. Figure 4 (b) and (c) show the separated diffuse component and specular component respectively. Both from the simulation and the experiment with real data, it is known that the proposed algorithm is effective and the computation is stable.

## 5. Conclusion

We have studied an approach for estimating reflectance properties by observing a real object and successfully separated the diffuse reflection component and specular reflection component from the real images. One of key features of the proposed approach is that we estimate reflectance

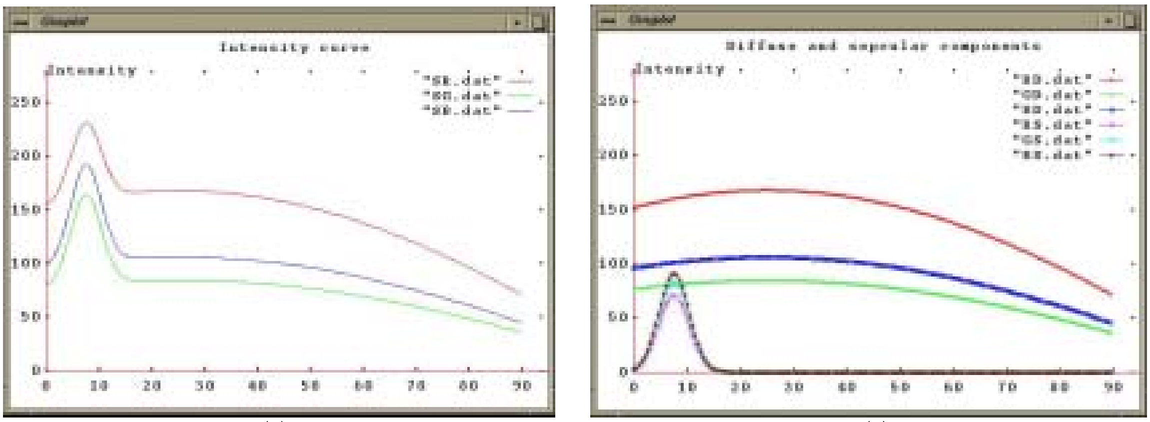


(a) (b)

Figure 3. Synthesized RGB data (a) and separated two components (b)

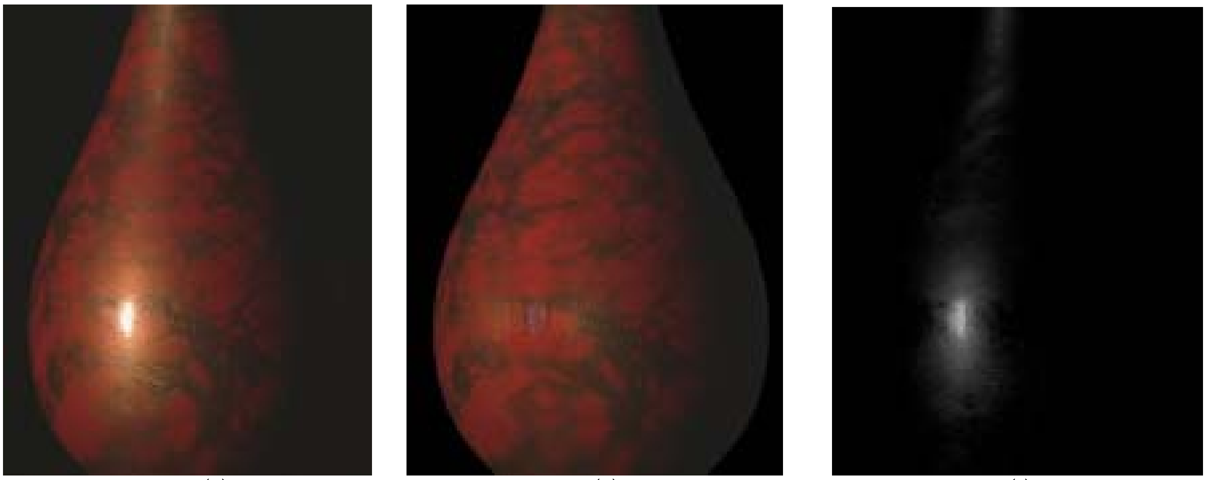

(a) (b) (c)

Figure 4. Original image (a); separated diffuse component (b) and specular component (c).

properties first before separation to eliminate error produced during separation; another feature is that we estimate both diffuse and specular parameters at the same time without knowing body color and light source color, which makes the proposed approach more effective and stable. We can observe that the proposed approach can be used for objects with complicated texture and with high specular reflectance. Generally it can be applied to any object shape if the sampled intensity data can be obtained. We also have noticed that the small area corresponding to the highlight in the diffuse component is not so natural due to the camera's dynamic range. At the current stage, the algorithm can only be used for environment with only one single point light source. In our future work, experiments with object shape and the multi-light source and area light source will be under our investigation.

## Acknowledgement

This work is one part of a project supported by TAO.

## REFERENCES

1) G. J. Klinger, S. A. Shafer and T. Kanade, "Using a color reflection model to separate highlights from object color", International Conference on Computer Vision, pp. 145-150, 1987.
2) G. J. Klinker, S. A. Shafer, and T. Kanade, "The measurement of highlight in color images", *International Journal of Computer Vision (IJCV)*, Vol. 2, No. 1, pp. 7-32, 1988.
3) G. J. Klinker, S. A. Shafer, and T. Kanade, "A physical approach to color image understanding", *International Journal of Computer Vision (IJCV)*, Vol. 4, No. 1 pp. 7-38, 1990.
4) S. K. Nayar, X. S. Fang, and T. Boult, "Separation of reflection components using color and polarization", *International Journal of Computer Vision (IJCV)*, Vol. 21, No. 3, pp. 163-186, 1997.

5) K. Ikeuchi and B. K. P. Horn, "Numerical shape from shading and occluding boundaries", *Artificial Intelligence*, Vol. 17, pp. 141-184, August 1981.
6) A. P. Pentland, "Local shading analysis", *IEEE Transactions on Pattern Analysis and Machine Intelligence,* Vol. PAMI-6, No. 2, pp. 170-187, March 1984.
7) K. Schluns, O. Wittig, "Photometric stereo for non-Lambertian surfaces using color information", *In proceedings of 7th International Conference on Image Analysis and Processing*, pp. 505-512, 1993.
8) R. J. Woodham, Y. Iwahori, and R. A. Barman, "Photometric stereo: Lambertian reflectance and light sources with unknown direction and strength", Technical Report 91-18, August 1991.
9) Y. Sato and K. Ikeuchi, "Temporal-color space analysis of reflection", *Journal of Optical Society of America A*, Vol. 11, No. 11, pp. 2990-3002, November 1994.
10) Y. Sato, M. D. Wheeler and K. Ikeuchi, "Object shape and reflectance modeling from observation", *SIGGRAPH'97*, pp. 379-387, 1997.
11) Zhengyou Zhang, "A flexible new technique for camera calibration", IEEE Transaction on Pattern Analysis and Machine Intelligence, Vol. 22, No. 11, pp. 1330-1334, November 2000.
12) K. E. Torrance and E. M. Sparrow, "Theory for Off-specular Reflection from Roughened Surfaces", *Journal of the Optical Society of America, (JOSA)*, No. 57, pp. 1105-1114, 1967.
13) W. H. Press et al., "Numerical recipes in C: the art of scientific computing", 2nd edition, Cambridge University Press, 1992.